

SOTERIA FINAL WORKSHOP

PREDICTION OF DOSE-DEPENDENT FRACTURE RESPONSE EVOLUTIONS BASED
ON MATERIAL MICROSTRUCTURE OBSERVATIONS IN RPV STEELS

27TH JUNE 2018

Contribution to SOTERIA WP5

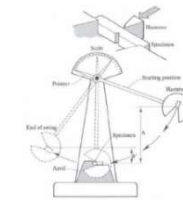
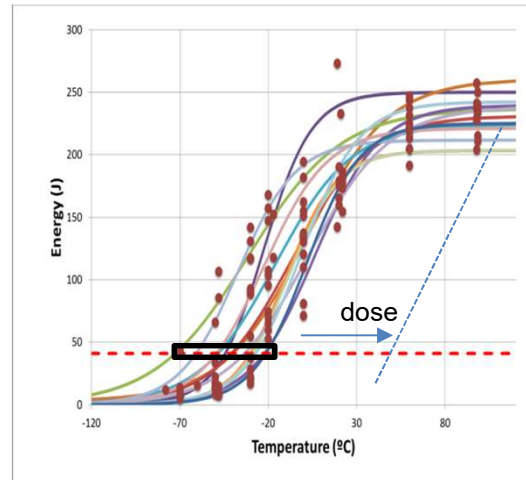
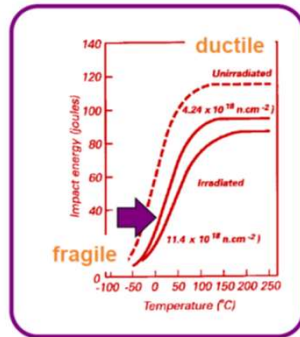
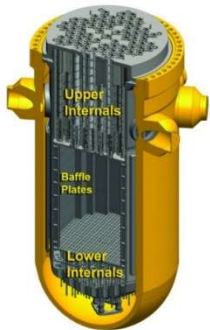
Co-workers: B. Marini, P. Forget, L. Vincent, Y. Li

Speaker: **Christian Robertson**

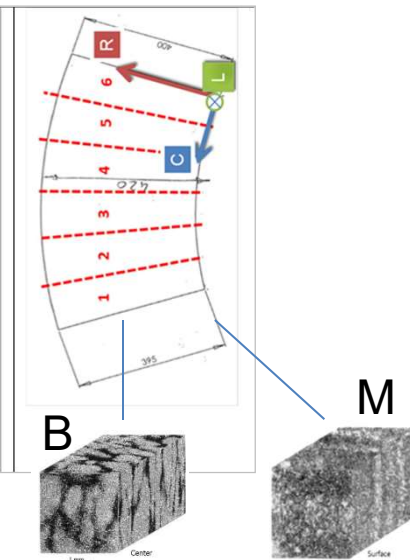
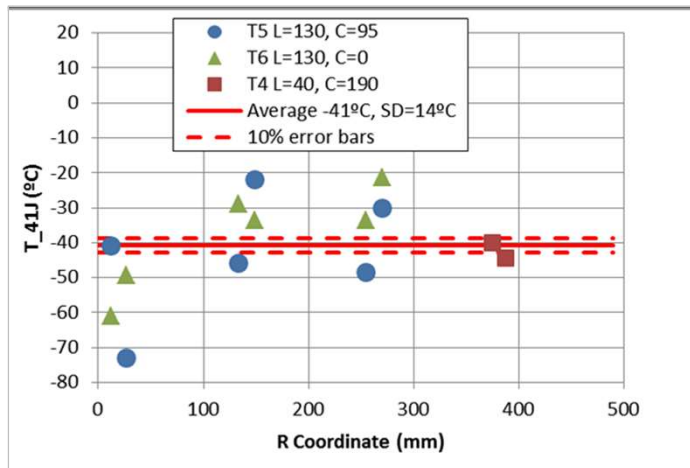
Fracture response of RPV steel forgings



Ductile to brittle transition temperature?

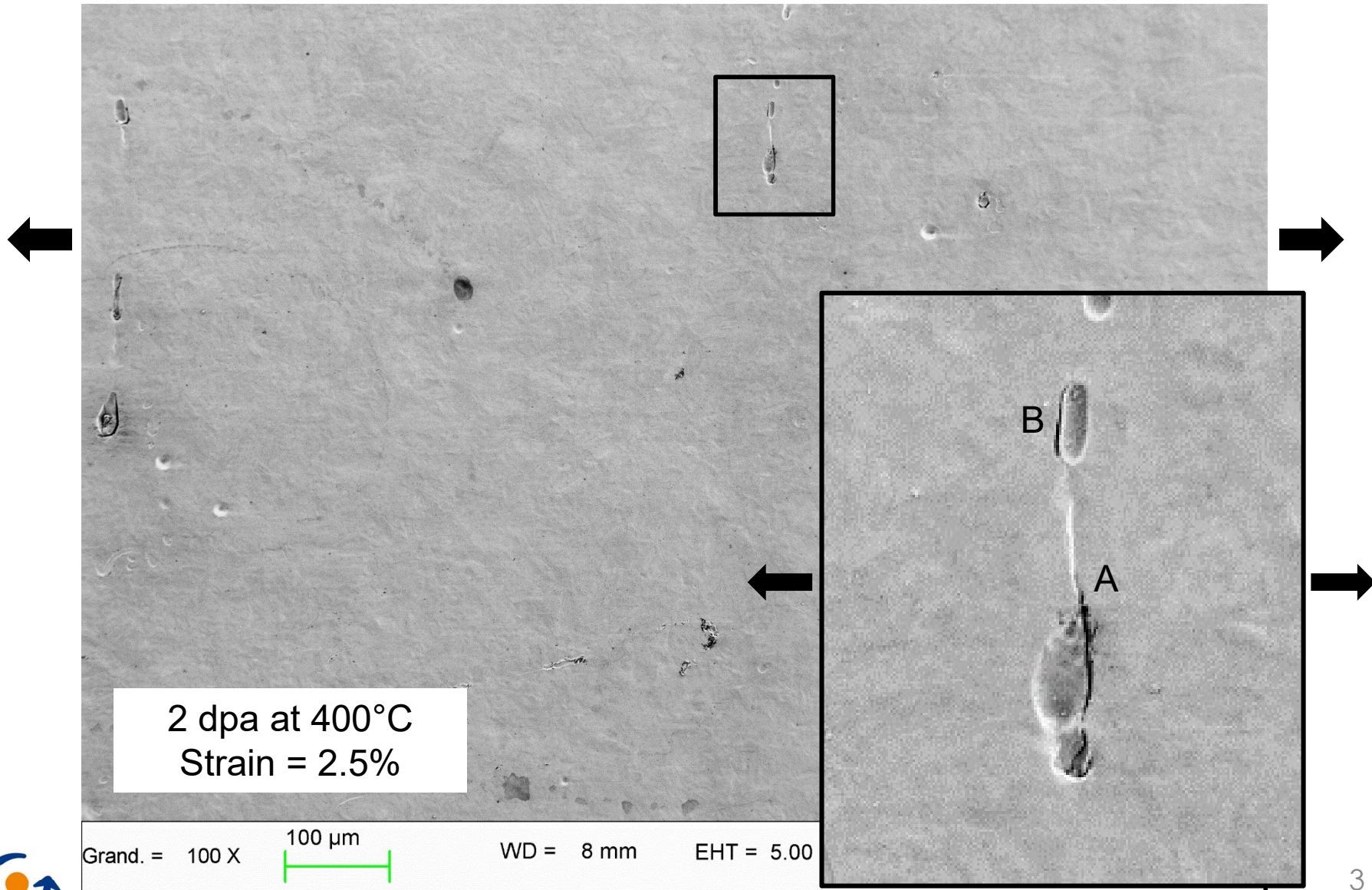


Significant data scattering in as-received condition



Data scattering persists in post-irradiated conditions

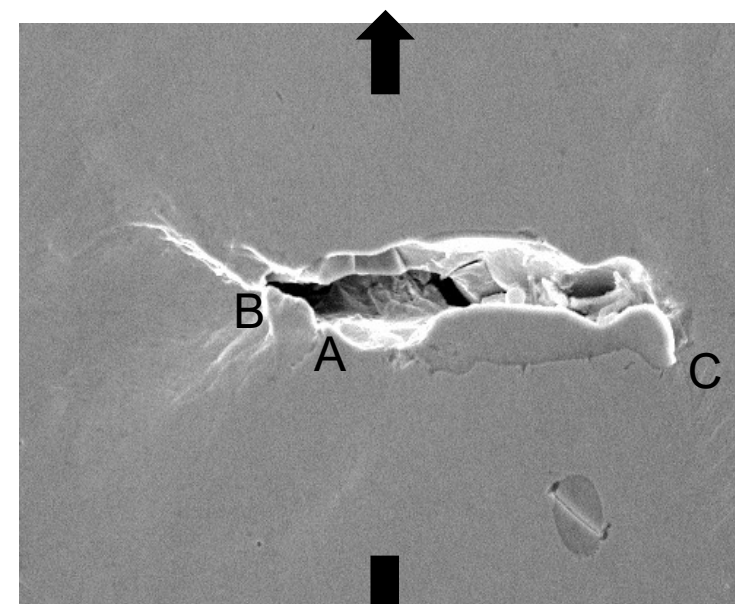
Micro-crack initiation



Resistance to micro-crack growth



$\epsilon_p = 2.5\%$



$\epsilon_p = 8\%$

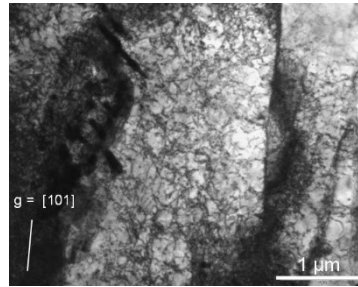
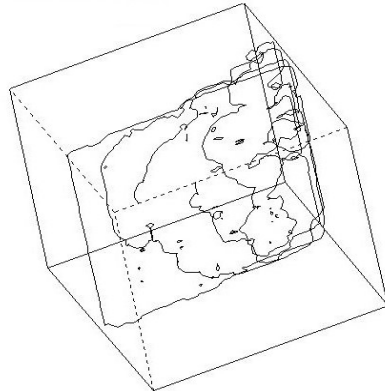
- Position A: poor resistance to crack growth (RCG) → few, thick shear bands, as crack A→B
 - Position C: strong resistance to crack growth → numerous, thin shear bands
- ☞ Plastic strain spreading in the matrix controls the materials Resistance to Crack Growth (RCG)
- ☞ Dose-dependent evolutions in the matrix → dose-dependent RCG

Dislocation dynamics simulations?



Q. Investigation of dose-dependent changes of plastic strain spreading?

Hard grain boundaries



$\epsilon_p = 8\%$

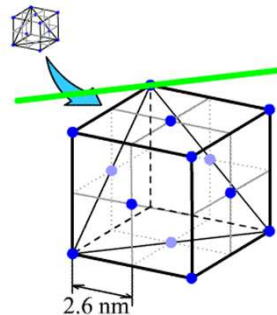


Initial FR sources

Tensile applied load

Quasi-static loading
Strain-rate controlled

DD code: dislocation mobility, multiplication, cross-slip, etc

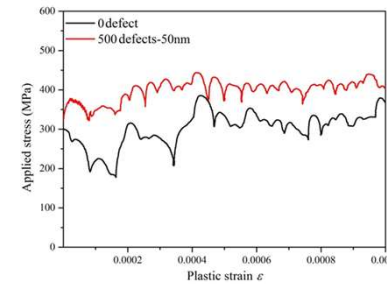


« TRIDIS » code

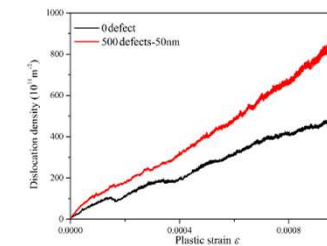
Model. Simul. Mater. Sci. Eng. 6 (1998) 755-770

27/06/2019

SOTERIA



Stress-strain response



Dislocation structures

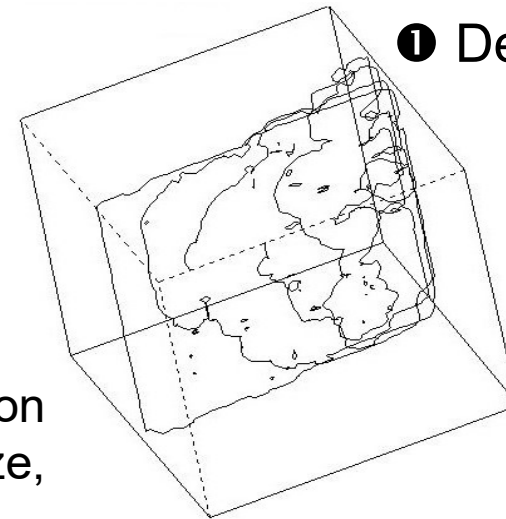
Post-Processing

Surface displacements
Local stress fields

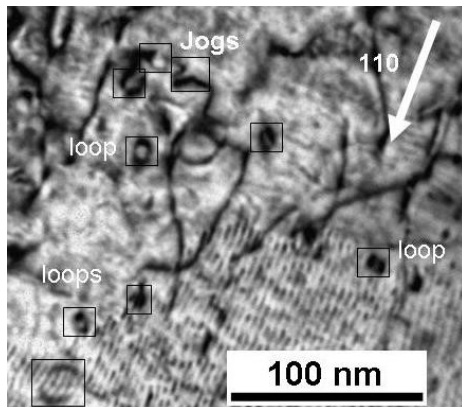
Discrete screw/edge lines
Discrete time step: 10^{-10} s
Discrete positions

1 μm^3 ferritic grains (Fe-C or Fe-Cr):

- Defect number density and defect size depend on selected dose and T_{irr} condition
- Uni-axial tension, strain-rate controlled conditions, fixed straining T° , presence of cross-slip
- **Model INPUTS:** grain size, kink-pair activation energy, phonon drag coefficient, irradiation defect size, and number density

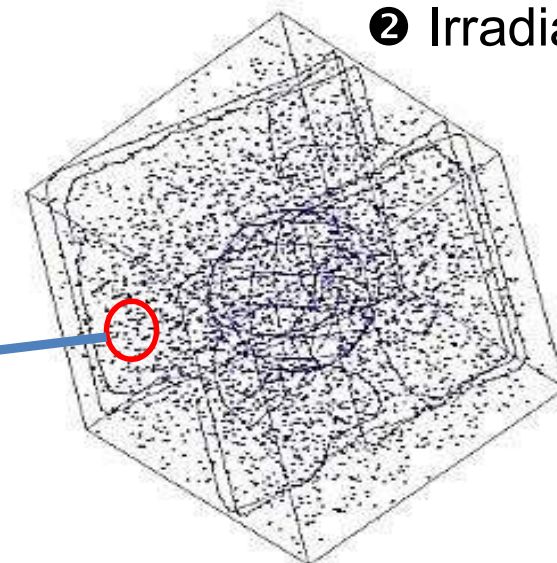
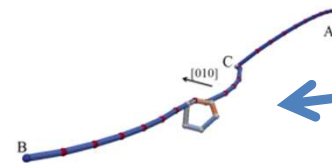


❶ Defect-free

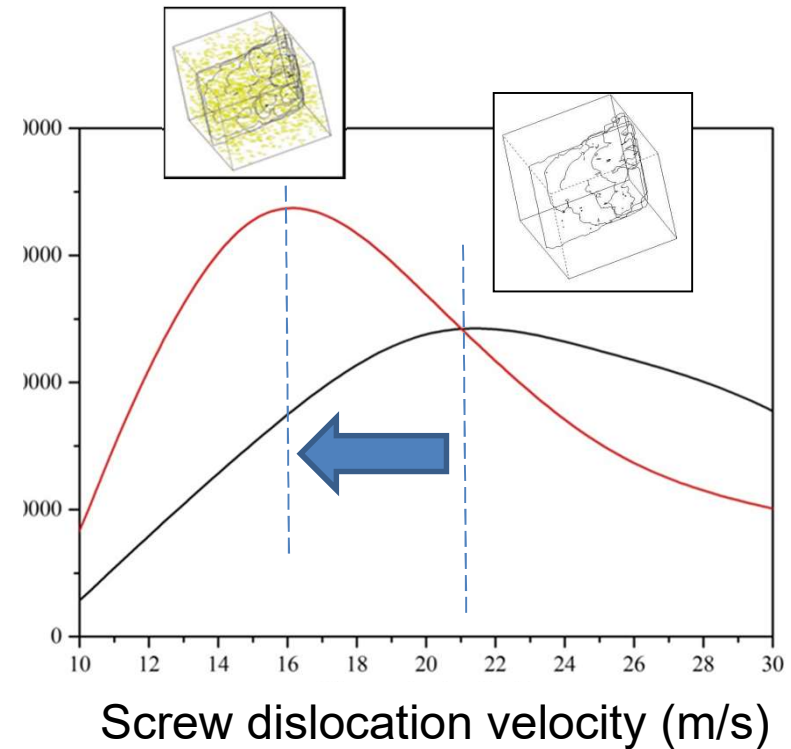
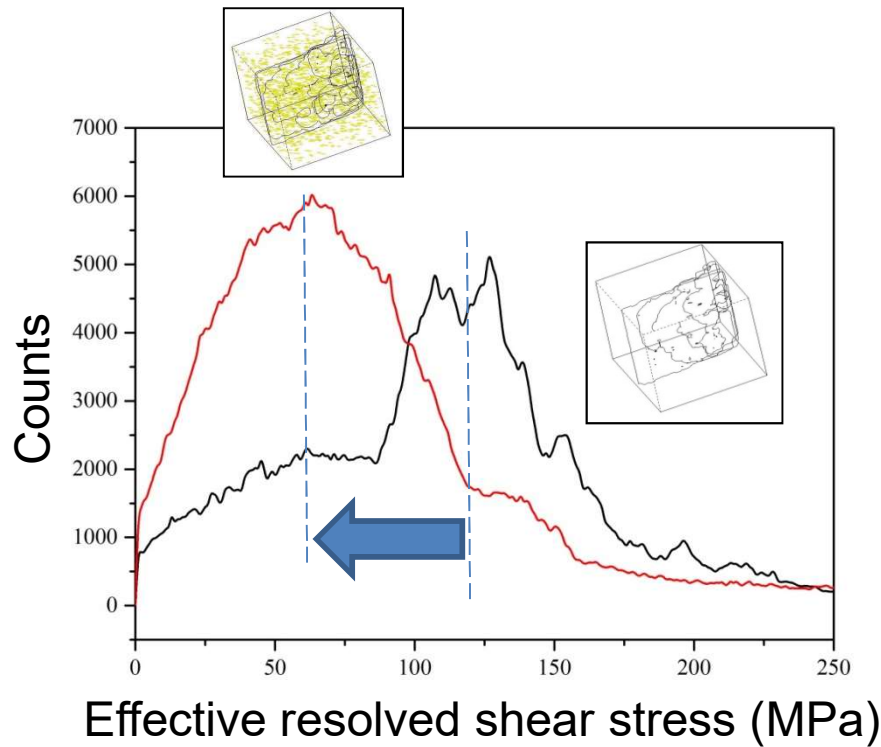


$T_{irr}=400^\circ\text{C}$, dose = 1 dpa, defect size $D = 50$ nm

dislocation/defect interactions

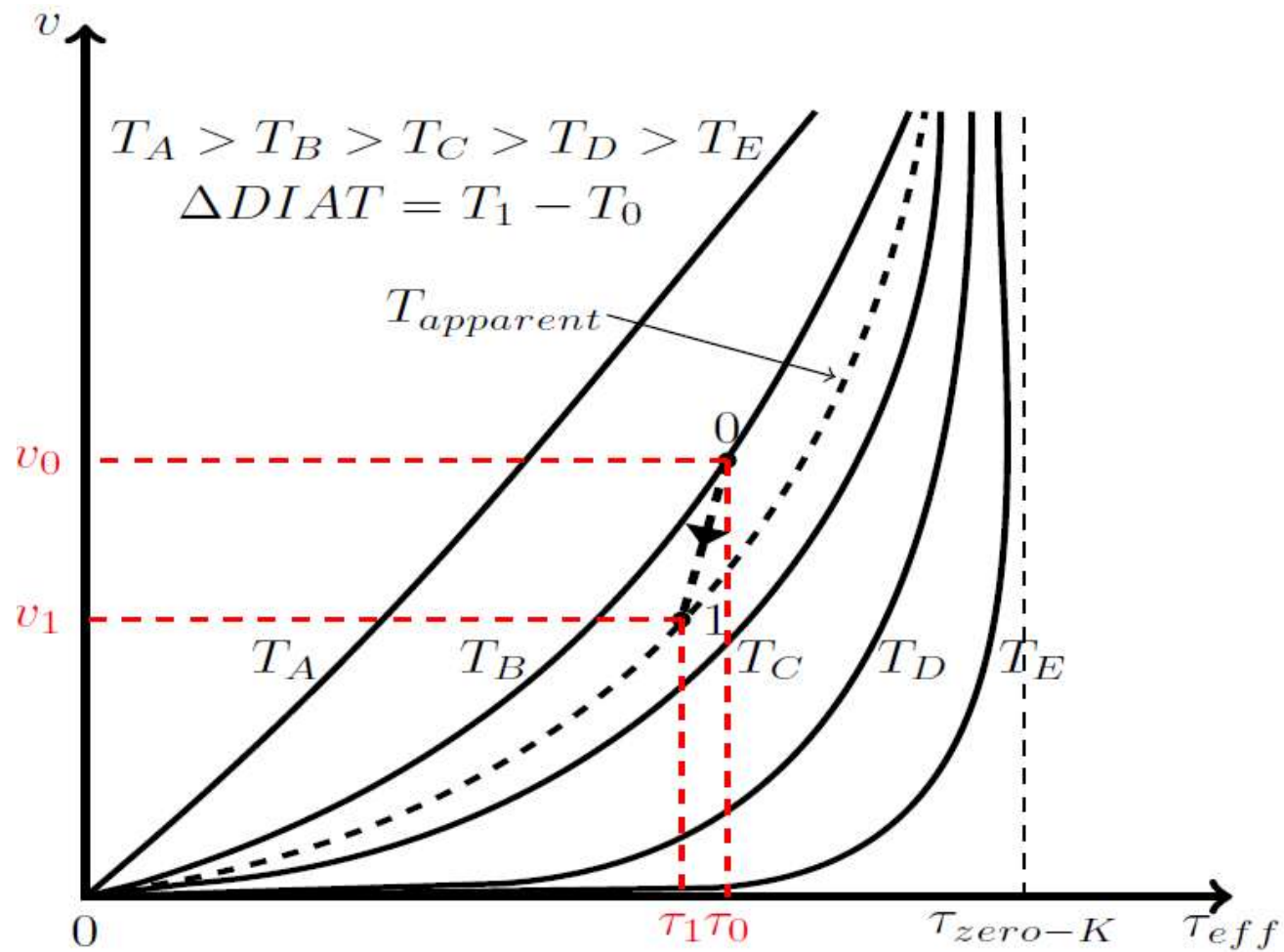


❷ Irradiated



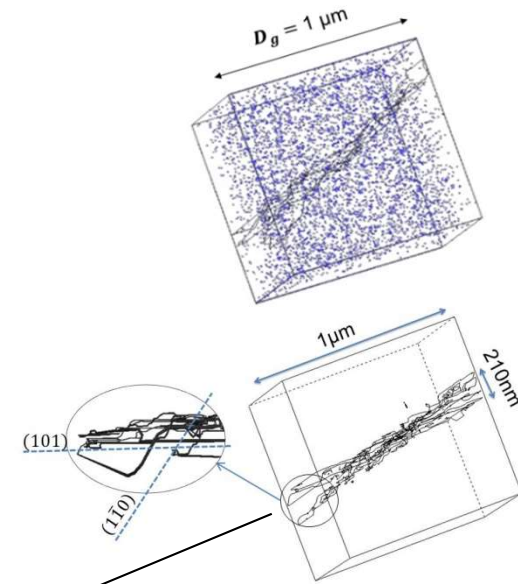
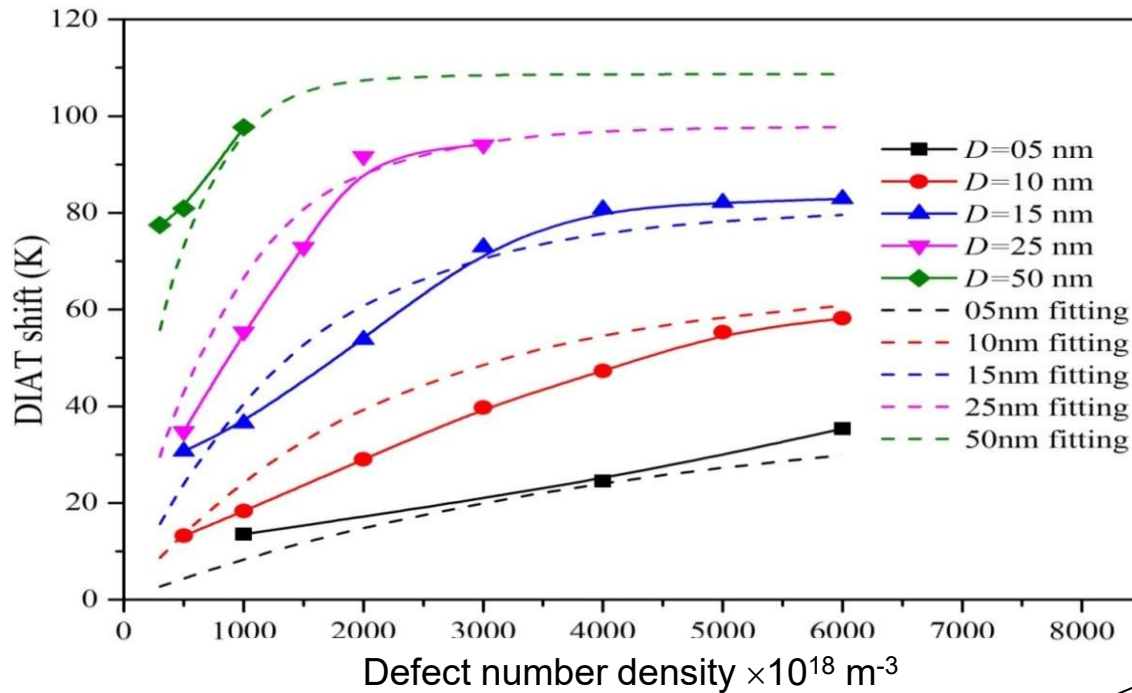
- Defect-induced effect on effective screw dislocation mobility : **statistically significant**. Why it matters?

DIAT shift: interpretation



$T_{apparent} - T_0 =$ Defect-Induced Apparent straining Temperature shift ($\Delta DIAT$)

ΔDIAT: a systematical investigation



$$\Delta DIAT = \Delta T_{max} \left(1 - \exp\left(-\frac{D}{\lambda}\right) \right) \left(1 - \exp(-d^2 DN) \right) \approx \Delta DBTT$$

N : defect number density (in nm⁻³); D : defect size (in nm);
3 material-dependent scaling parameters (ΔT_{max} , d and λ)

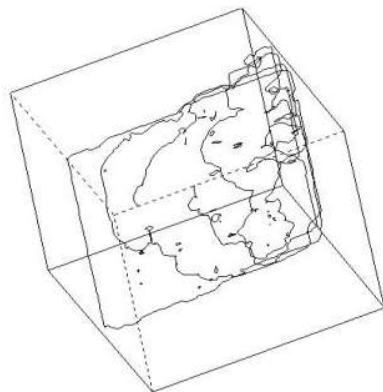
Δ DIAT: a simple, predictive DBT shift indicator



$$\Delta \text{DBTT} \approx \Delta \text{DIAT} = \Delta T_{max} M$$

ΔT_{max} → first principles
elasticity theory &
dislocation statistics

- ΔH_0 (Joules)
- τ_{Peierls} (MPa)
- μ (MPa)
- B (MPa.s)
- T_0 (K)
- [n] and D at saturation
- effective τ_1 (Orowan)
- effective τ_0 (at $T_0 = 300\text{K}$)**
- No adjustable variable/parameters



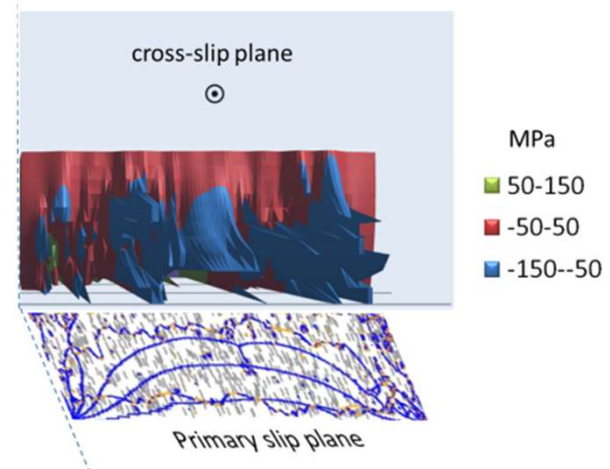
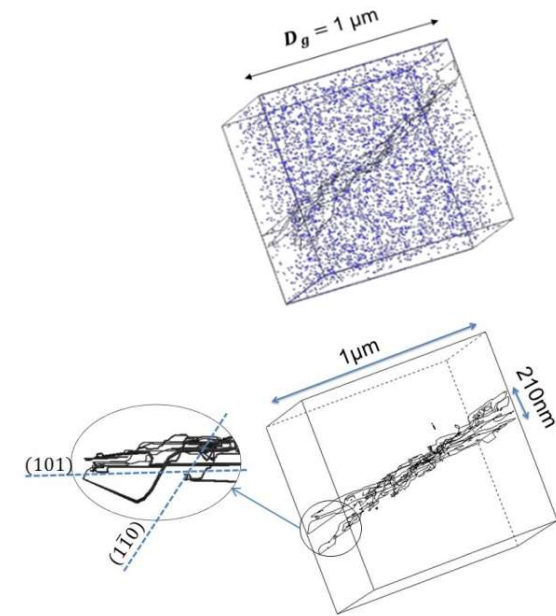
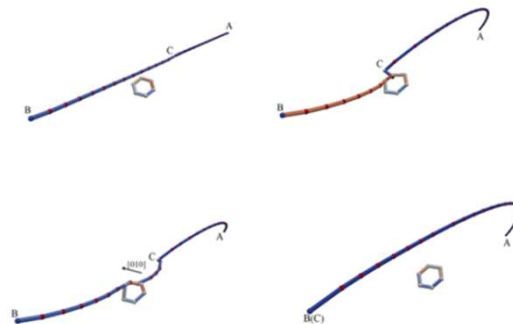
$0 < M < 1$:
dimensionless «mitigation» term



$M \propto$ «stress landscape» associated
with shear band structures



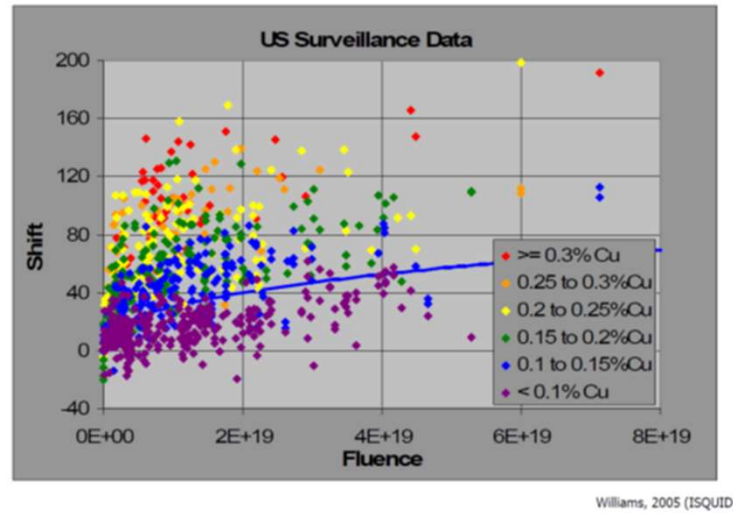
Controls cross-slip activity →
effective defect interaction strength
(τ^*) and dislocation length (X')



Δ DIAT/ Δ DBTT comparison: data collection



Dose-dependent DBT shift



Defect number density

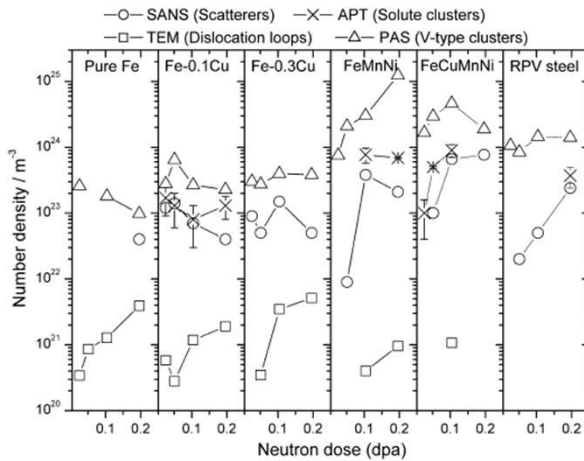
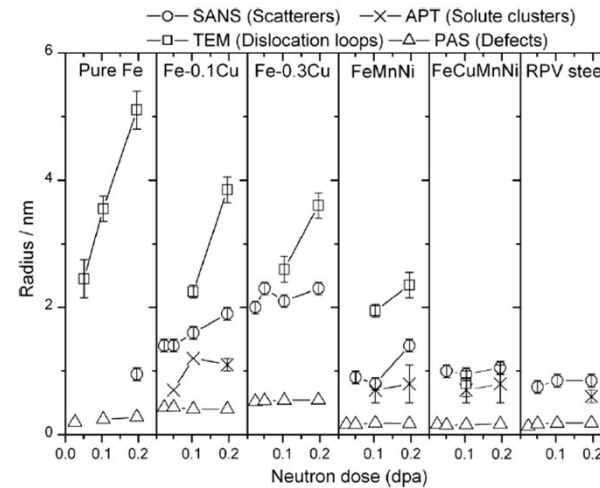


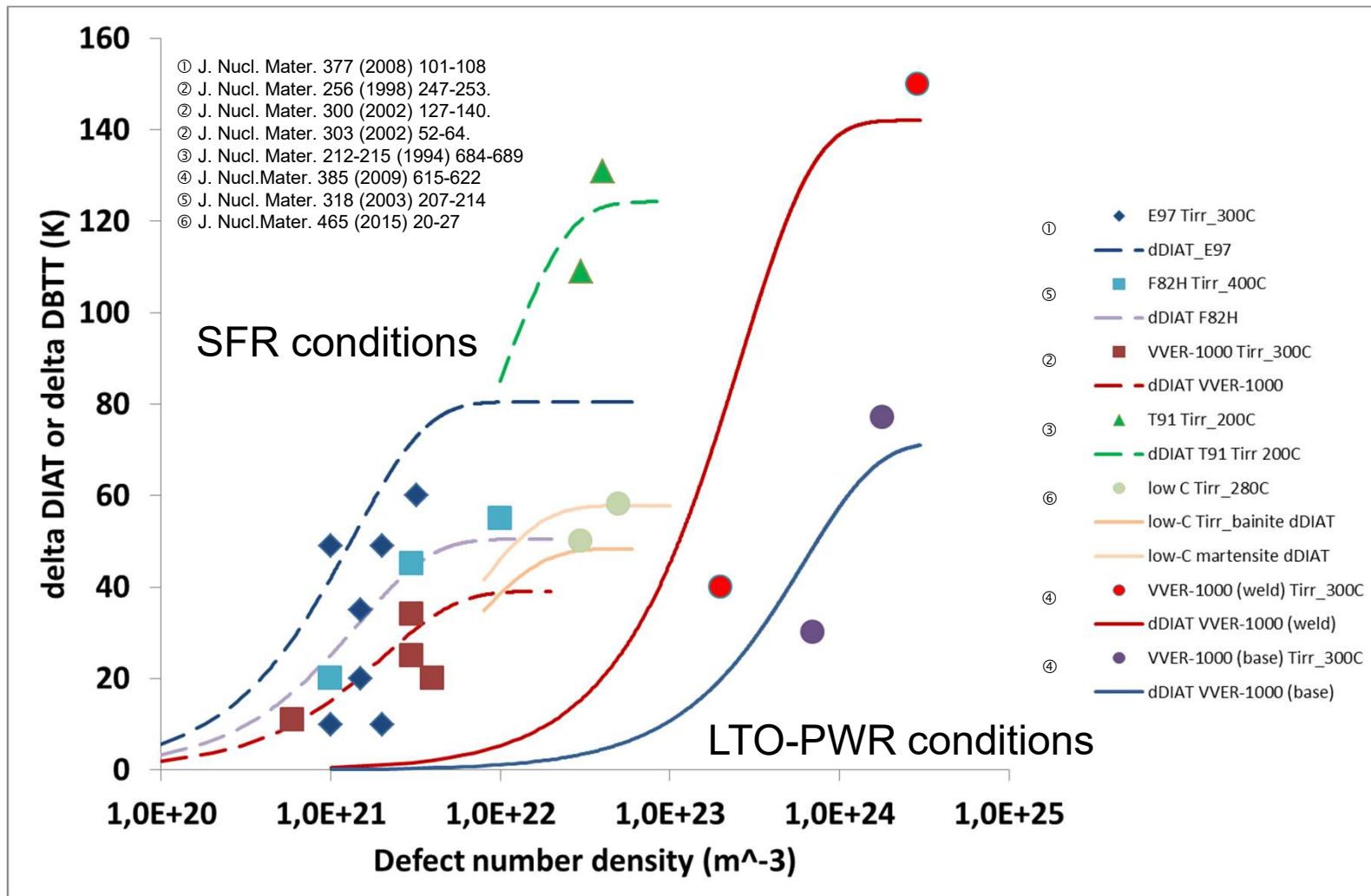
Fig. 3. Number density of radiation-induced damage as functions of dose from APT, SANS, TEM and PAS measurements.

Defect size



Journal of Nuclear Materials 406 (2010) 84-89

Δ DIAT/ Δ DBTT comparison

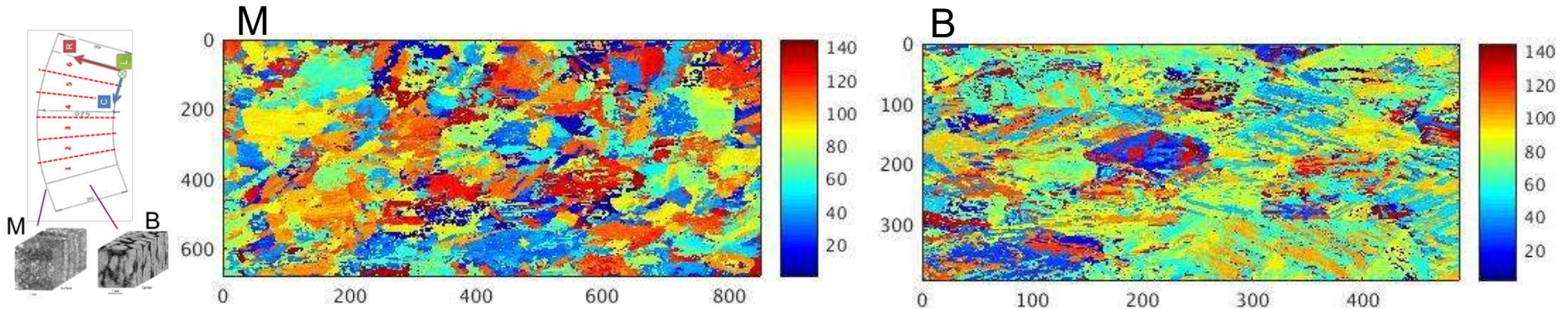


- ☞ Δ DIAT \approx Δ DBTT [irradiation conditions: little or no segregation at fracture initiators (particles or GB)]
- ☞ Absolute toughness levels: link with local approach of fracture/MIBF approach/models
- ☞ Support/link dose-dependent crystal plasticity...

IV-Application: post-irradiation fracture response analysis of 2 model materials

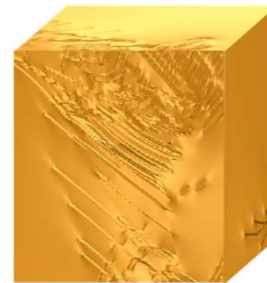
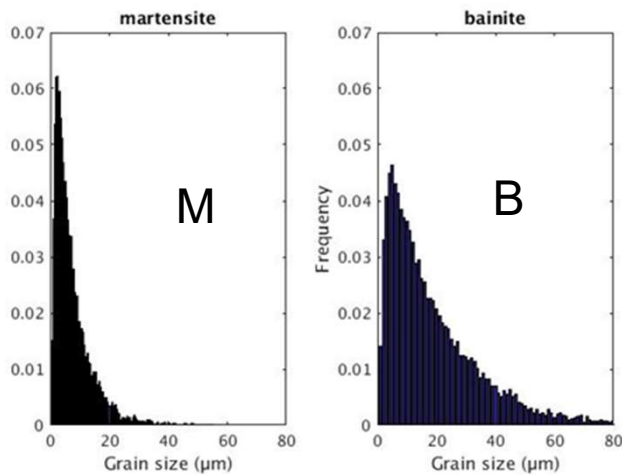


EBSD: grain orientation maps ↗ 2 model materials (Martensite&Bainite), same chemical composition



B. Marini et al. JNM 465 (2015) 20-27

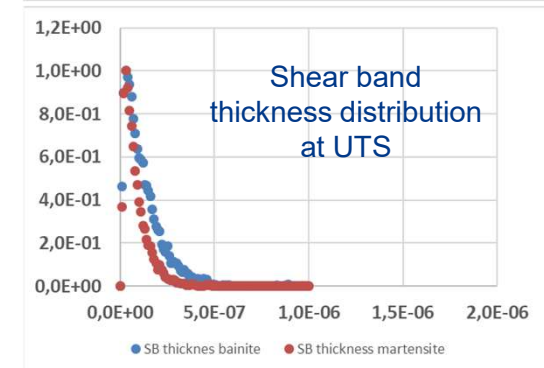
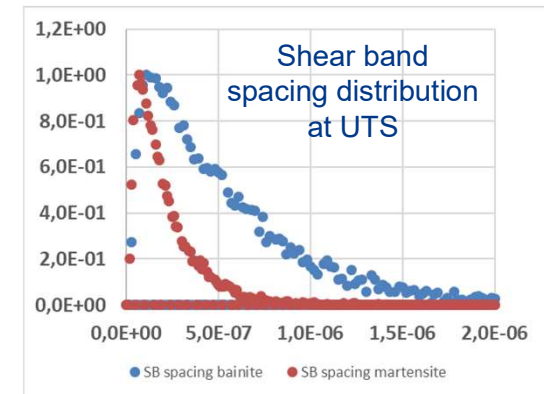
Grain size/orientation distributions



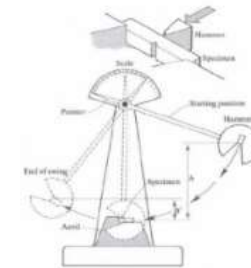
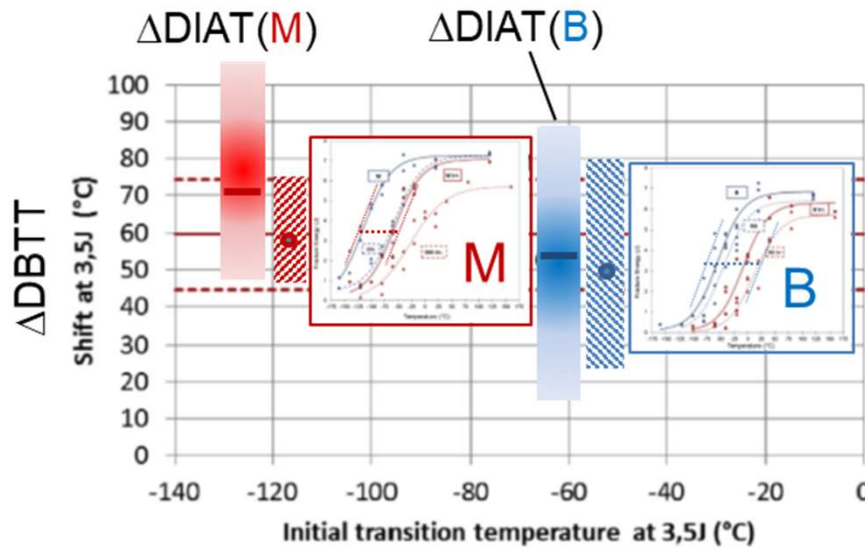
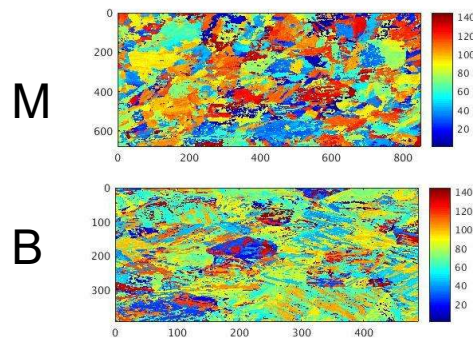
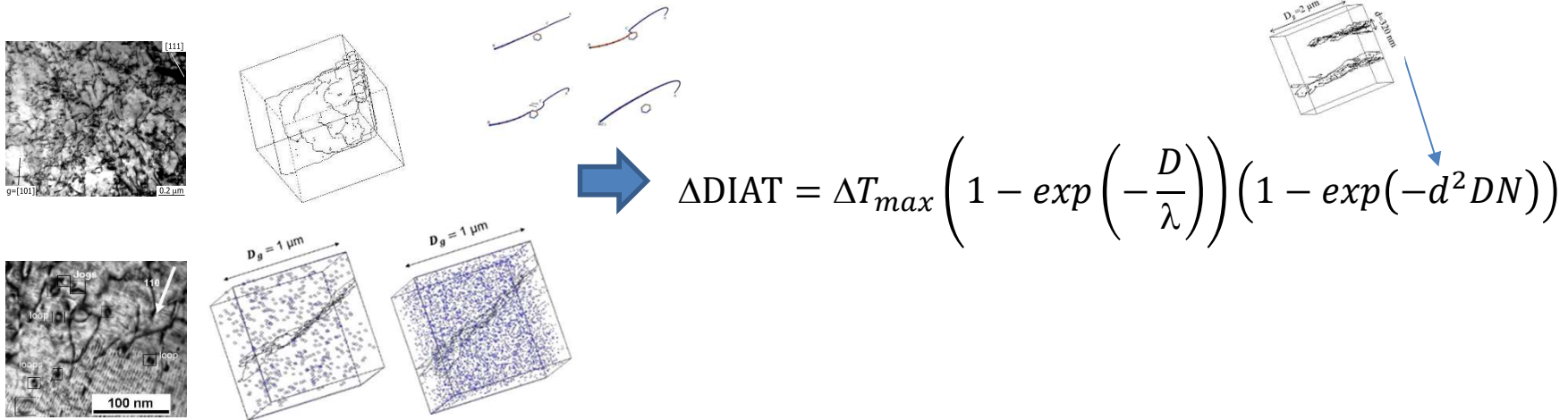
Neutron irradiation
0.1 dpa, 290°C



Defect size & number density



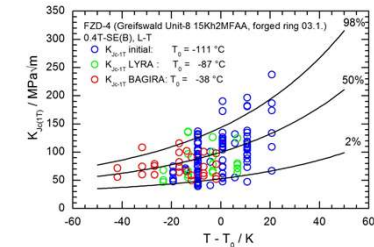
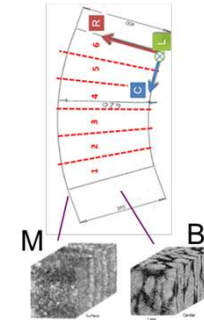
IV-Validation: DIAT/DBTT comparison



DIAT: estimation de la fragilisation induite par l'irradiation / mesures non-destructives

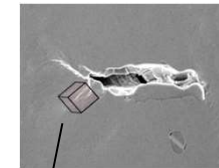
RPV steel forgings include different position-dependent microstructures

Initial RPV steel heterogeneities ↔ fracture data scattering, in both as-received and post-irradiated conditions



Dose-dependent fracture response evolutions: DIAT concept

- ☞ Δ DIAT level characterizes plastic strain spreading around micro-crack initiators (inclusions or GB)
- ☞ Δ DIAT \sim Δ DBTT in a broad range of irradiation conditions (defect size and number density)



$$\Delta \text{DIAT} = \Delta T_{max} \left(1 - \exp\left(-\frac{D}{\lambda}\right) \right) \left(1 - \exp(-d^2 DN) \right)$$

Evaluation of dose-dependent fracture response using non-destructive testing

- ☞ Time and cost effective procedure; support to conventional surveillance programs
- ☞ Adapted to actual, heterogeneous structural materials, including weld joints

Thanks for your attention

Questions?

FCC models (Cu, FCC Fe)

Screw ~ Edge

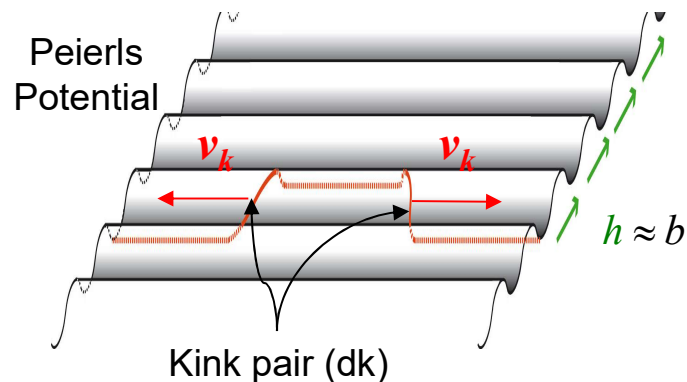
Negligible Peierls barrier ($\tau_p \sim 10$ MPa)



Phonon-drag mechanism

$$v_{screw}(\tau) = v_{edge}(\tau) = \frac{\tau b}{B}$$

- τ : applied stress $\gg \tau_p$
- B : Viscous drag coefficient
- b : Burgers vector module
- τ_p : Peierls Stress



BCC Fe and Fe alloys

Screw \neq Edge

Velocity anisotropy depends on T°

Low temperature

High temperature

Significant Peierls barrier ($\tau_p \sim 1$ GPa)

Athermal regime



Thermally activated mobility

$$v_{screw}(\tau, T) \ll v_{edge}(\tau) = \frac{\tau b}{B}$$

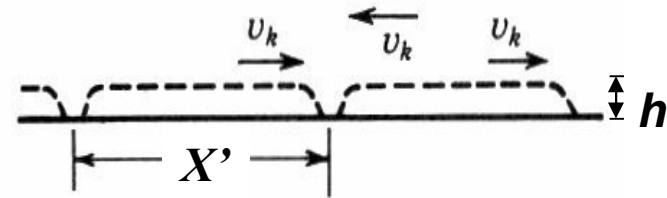
$$v_{screw} \approx v_{edge}$$

Low-T screw dislocation mobility mechanism

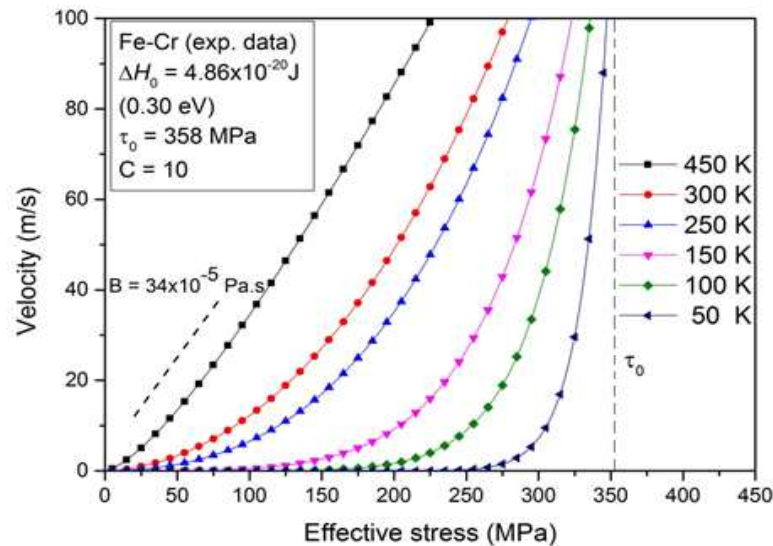
- **Nucleation** of a kink pairs (thermally activated)
- Kink pair **propagation** $v_k \propto \tau$ « effective » $B_k < B_{edge}$

Journal of Nuclear Materials 504 (2018) 84-93

$$v_{screw} = hJX'$$



- h : distance between Peierls valleys
- J [$\text{m}^{-1}\text{s}^{-1}$] : kink pair **nucleation rate** per unit length
- X' [m] : kp **mean free path** before annihilation with another dk
[increases with kink velocity (v_k) and decreases with J]



$$v_{screw}(\tau^*, T) = \underbrace{\frac{8\pi b(\tau^*)^2}{\mu Bh}}_{\text{Stress-dependent pre-factor}} X' \exp\left(-\frac{\Delta G(\tau^*, T)}{k_B T}\right)$$

Stress-dependent pre-factor

☞ Progressive transition from Low- T to Room- T

Δ DIAT: a simple, predictive DBT indicator



Stress landscape \leftrightarrow shear band spreading

Grain size and grain orientation
Dose-dependent τ_{YS} (MPa)
Strain per shear band
 $[\eta]$ and D at considered dose, irradiation- T°
Defect strength (MPa)
Dislocation accumulation rate with ϵ_p

Shear band spacing and thickness: micro-model based on **DD simulation results**



Micro-model validation based on comparison with experimental observation of strained specimens

